Research Article

Zhilin Cao, Changxin Ren, and Zhengzhou Wang*

Copper phenyl phosphonate for epoxy resin and cyanate ester copolymer with improved flame retardancy and thermal properties

https://doi.org/10.1515/epoly-2023-0004
received January 26, 2023; accepted April 22, 2023

Abstract: Epoxy resin (EP)/cyanate ester (CE) copolymer, an important structural material with high temperature resistance and low dielectric constant in aerospace, microelectronics, and related fields, is still of great flammability danger. In this work, copper phenyl phosphonate (CuPP), a flame retardant used in EP/CE copolymer was synthesized by the reaction of phenyl phosphonic acid and copper nitrate trihydrate. The fire and thermal behavior of EP/CE/CuPP composites were studied in detail. The results suggested that the UL-94 rating and limiting oxygen index of EP/CE composite with 5 wt% CuPP (EP/CE/CuPP5) reach V-1 level and 30.6%, respectively. Compared with pure EP/CE copolymer, the peak heat release rate and total heat release values of EP/CE/CuPP5 decreased by 34.5% and 18.9%, respectively. The glass transition temperature of EP/CE/CuPP composite is higher than that of pure EP/CE copolymer, suggesting that the fire-retardant composite has higher work temperature and better heat resistance.

Keywords: copper phenyl phosphonate, epoxy resin, cyanate ester, flame retardant, thermal properties

1 Introduction

Epoxy resin (EP) is widely used in many industrial fields due to its excellent comprehensive properties, such as adhesion, chemical resistance, and mechanical properties. However, due to the existence of some strong polar groups, such as hydroxyl group, the dielectric properties of EP resin are not enough to meet the special requirements for high-speed electronics. The cyanate ester (CE) resin has outstanding heat resistance and low dielectric constant; therefore, it is usually used to improve the related properties of EP resin (1–6). For example, Kim studied the curing behavior and thermal stability of EP/CE copolymers and found that the curing reaction of EP/CE copolymer was faster than that of pure EP resin and the initial decomposition temperature of the copolymer was raised with the increase of CE content (7). Similarly, Jayakumari et al. (8) observed that with the increase of CE content, the mechanical strength of EP/CE copolymer was increased, and the thermal stability of the copolymer also was improved. Liang and Zhang (9) found that the processability of CE resin was improved via copolymerization with EP resin, and the modified resin had excellent dielectric properties. Lin (10) found that the incorporation of phosphorus element into CE, which was a frequent way to improve the flame retardancy of resin, would not sacrifice the dielectric properties.

Although EP/CE copolymer has low dielectric properties and good heat resistance, it is still of great flammability danger. Traditional halogen-containing flame retardant produces a great deal of smoke and toxic substances during burning; thus, its application is restricted in some fields, especially in the electronic and electrical fields (11). There is some research on the halogen-free flame retardancy of EP/CE copolymer. For example, Ho (12) found that, compared with the control pure EP resin, the EP/CE composites with 2-(6-oxido-6*H*-dibenz(*c*, *e*)(1,2)-oxaphosphorin-6-yl)-1,4-benzenedio (containing 2 wt% phosphorus content) have better flame retardancy and higher glass transition temperature (T_g). Toldy et al. (13) successfully prepared the copolymer containing bisphenol-A diglycidyl ether and phenolic CE, modified the copolymer by 9,10-dihydro-9-oxa-10-phosphazephenanthrene-10-oxide (DOPO), and then found that the EP/CE/DOPO composites

* **Corresponding author: Zhengzhou Wang,** Department of Polymeric Materials, School of Materials Science and Engineering, Tongji University, Shanghai 201804, China; Key Laboratory of Advanced Civil Engineering Materials of Ministry of Education, School of Materials Science and Engineering, Tongji University, Shanghai 201804, China, e-mail: zwang@tongji.edu.cn
Zhilin Cao, Changxin Ren: Department of Polymeric Materials, School of Materials Science and Engineering, Tongji University, Shanghai 201804, China

with 2 wt% phosphorus content reach UL-94 V-0 level. Our team (14) enhanced the flame retardancy of EP/CE composite by adding the compound of DOPO and wollastonite (Wo) and reported that the EP/CE composites with 7 wt% DOPO and 3 wt% Wo reached UL-94 V-0 level with LOI of 35.5%.

However, the difficulties of halogen-free flame-retardant research for EP/CE copolymer are concentrated mainly on the high curing temperature (more than 200°C) and active groups (i.e. –OH and $-NH_2$) affecting the curing reaction, which restricts the application of most halogen-free flame retardants in this system. Moreover, the majority of halogen-free flame retardants generally result in a reduction in the thermal stability of EP/CE composites, such as T_g (13,15).

Metal organic phosphates have received great concern in the research on flame retardant for polymers because of their water insolubility and good compatibility with polymer matrix. Müller and Schartel (16) compared the flame retardancy of three metal organic phosphates (MPAlP, MPZnP, and MPMgP) in EP and found that the three composites containing them (20 wt%) showed at least a 50% reduction in PHRR, while a reduction in smoke and carbon monoxide generation and an increase in the amount of fire residue were observed. Liu and colleagues (17) synthesized metal-phosphorus hybrid nanomaterials with various metal centers (Al, Zn, and Fe) through a hydrothermal reaction between metal hydroxides and phosphite/phosphonic acid. It was found that the addition of metal organic phosphates significantly improved the flame retardancy of the EP, while according to the TG-IR results, the increase in flame retardancy is likely to be due to the delayed release of the flammable components resulted from the metal centres of the metal organic phosphates. And in our recent work (18), a metal organic phosphonate (CuPB) was synthesized and used to modify EP, and the EP composite with only 3.0 wt% CuPB can pass the UL-94 V-0 rating. However, there are few reports on the use of metal organic phosphates in EP/CE copolymer.

Herein, copper phenyl phosphonate (CuPP) was successfully synthesized via simple method. The burning behaviors of EP/CE/CuPP composites were evaluated by LOI, UL-94, and cone colorimeter test. Moreover, the thermal and mechanical properties were studied.

2 Materials and methods

2.1 Materials

Copper nitrate trihydrate ($Cu(NO_3)_2{\cdot}3H_2O$, A.R.), deionized water, absolute ethanol, and sodium hydroxide (NaOH, A.R.) were obtained from Sinopharm Group Chemical Reagent Co., Ltd (China). Phenyl phosphonic acid (PPA, A.R.) was supplied by Aladdin Reagent Co., Ltd (China). Bisphenol-A dicyanate ester (CE) resin was purchased from Jiangsu Wuqiao Resin Plant (China). Diglycidyl ether of bisphenol-A epoxy resin (EP) with an epoxy equivalent weight of 186 g/eq was provided by Sinopec Group Company (China).

2.2 Preparation of CuPP

0.1 mol PPA was dissolved in 100 mL of deionized water. Then, 100 mL of $Cu(NO_3)_2{\cdot}3H_2O$ aqueous solution (1 mol·L^{-1}) was added dropwise under vigorous stirring and the pH value of the mixture was remained about 5 via the addition of NaOH. Then, the mixture was stirred at room temperature for 24 h. The precipitate was centrifuged and washed several times with deionized water and dried at 105°C for 24 h. Finally, the products were ground and sieved to obtain CuPP powder (200 meshes).

2.3 Preparation of EP/CE and its composites

Different amounts of CuPP were added into EP and CE solution (molar ratio of EP and CE = 1:1) were blended under vigorous stirring at 150°C for 1.5 h and then degassed in a vacuum oven at 150°C for 5 min. Subsequently, the mixture was poured into a Teflon mold and cured by the following protocol: 150°C for 2 h, 180°C for 2 h, 200°C for 2 h, and 220°C for 2 h. The synthesis recipe of the EP/CE/CuPP composites is listed in Table 1.

2.4 Characterization

Fourier transform infrared (FTIR) spectra were collected between 400 and 4,000 cm^{-1} using an EQUINOX 55 (Bruker,

Table 1: Formulations of EP/CE and its composites

Sample code	Component (wt%)	
	EP/CE*	CuPP
Pure EP/CE	100	0
EP/CE/CuPP3	97	3
EP/CE/CuPP5	95	5
EP/CE/CuPP7	93	7

*EP:CE = 1:1 (molar ratio).

Germany) by the KBr tablet method. X-ray diffraction (XRD) spectrum of CuPP was carried out on a D/MAX 2550VB3 X-ray diffraction spectrometer (Nippon Electric Motor, Japan) at a scanning speed of 5°·min^{-1}, ranging from 3° to 80°. Transmission electron microscope (TEM) graph of CuPP was carried out on JEM-2100F transmission electron microscope (Nippon Electric Motor, Japan). Scanning electron microscope (SEM) graphs were obtained by an S-2360 N instrument (Hitachi, Japan) with an electron high-tension voltage of 10 kV. The surface of the specimens was pre-treated with the gold spray to increase conductivity and prevent charge accumulation. Raman spectroscopic analysis was performed by a LabRAM HR Evolution laser confocal Raman spectrometer (HORIBA, France) with a laser wavelength of 532 nm. Thermogravimetric analysis (TGA) measurements were performed via a STA 6000 thermal gravimetric analyzer (PerkinElmer, USA) from 100°C to 700°C at a scan rate of 10°C·min^{-1} under nitrogen. The test sample mass was 10 ± 1 mg. Differential scanning calorimeter (DSC) analysis was carried out on a Q100 differential scanning calorimetry (TA, USA), and the samples of 7 ± 1 mg were heated from 50°C to 300°C with a heating rate of 10°C·min^{-1} under nitrogen. Each material was subjected to two measurements, and the results were averaged.

The fire behavior of the EP/CE copolymer and its composites were studied by LOI test, UL-94 burning test, and cone calorimeter test (CCT). LOI was measured on HC-2 Oxygen Indexer (Jiangning, China) according to GB/T 2406-2009 with the form IV sample size of 100 mm × 6.5 mm × 3 mm. UL-94 test with the sample size of 125 mm × 13 mm × 3 mm was performed on CFZ-3 instrument (Jiangning, China) in accordance with GB/T 2408-2021. CCT was tested in a cone calorimeter (FTT, UK) with the sample size of 100 mm × 100 mm × 3 mm at a heat flux of 35 kW·m^{-2} according to ISO 5660-1. Samples for LOI and UL-94 tests were measured fifth and those for CCT were measured twice; their average results were obtained.

The tensile strengths were measured by CMT5105 universal testing machine (MTS, USA) according to GB/T 1040-2006 by using type 1A dumbbell-shaped samples with an overall length of 170 mm, a gauge length of 50 mm, and a thickness of 4 mm. The impact strengths were measured according to GB/T 1043-2008 by SANS E21 pendulum impact testing machine (SANS, China) with the sample size of 80 mm × 10 mm × 4 mm. Five specimens of each material were measured in the tensile and impact strength tests, respectively.

3 Results and discussion

3.1 Characterization of CuPP

Figure 1a presents the FTIR spectrum of CuPP and PPA. As shown in Figure 1a, the absorption peaks in 2,000–1,600 cm^{-1} are related to the C–H stretching vibration of the benzene ring. The peak at 1,431 cm^{-1} corresponds to the absorption of the P–C bond. The strong peaks near 1,014 and 934 cm^{-1} are due to the stretching vibration of the P–O bond. The above results agree with the infrared results of phenyl phosphonates in the literature (19). In addition, the coordination between PPA and copper ion in CuPP can be proved from three aspects: the disappearance of P–OH peak in 2,700–2,560 cm^{-1} (20), the shift of P═O peak (from 1,220 to 1,186 cm^{-1}), and the appearance of peak at 1,031 cm^{-1} (21). Figure 1b shows the XRD graph of CuPP. Three strong diffraction peaks at 2θ = 5.68°, 11.44°, and 17.22° correspond to the (010), (020), and (030) crystal planes of CuPP, respectively (19,22). The above results indicate that CuPP was successfully synthesized. Figure 1c shows the TEM image of CuPP. The microstructure of CuPP presents a lamellar structure, which possibly increases the physical barrier effect of the char. Obviously, the thermal decomposition of CuPP has three steps. Before 300°C, CuPP has nearly no weight loss (only 0.54 wt%) and the temperature at 5 wt% mass loss ($T_{5\%}$) is 379°C, indicating that CuPP has high initial thermal stability. The first step occurring between 300 and 400°C with a weight loss of 5.76 wt% is attributed to dehydration and condensation of phosphonic acid groups. The mass loss at the second step in the range 400–500°C is related to the oxidation of some phosphorus group and the formation of $Cu_2P_2O_7$ (21,23) while the pyrolysis of benzene rings occurs when the temperature is higher than 500°C (24).

3.2 Fire behavior of EP/CE and its composites

3.2.1 LOI and UL-94

The flame retardancy of EP/CE and its composites is preliminarily evaluated through LOI and UL-94 vertical burning test and the results are arranged in Table 2. The pure EP/CE has an LOI value of 25.7% and no UL-94 test rating. The LOI values of EP/CE/CuPP3, EP/CE/CuPP5, and EP/CE/CuPP7

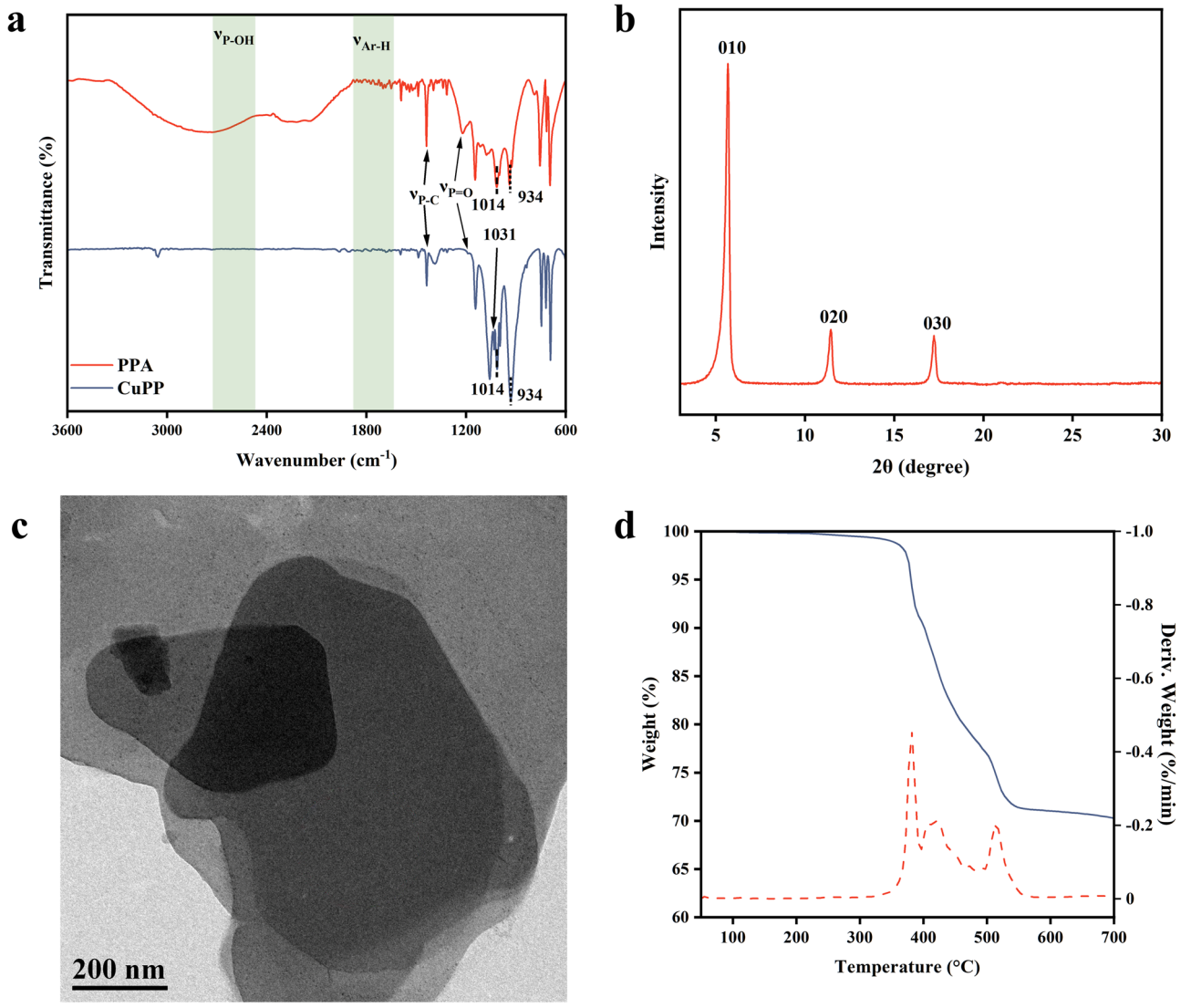

Figure 1: Characterization of CuPP: (a) FTIR spectra, (b) XRD pattern, (c) TEM, and (d) TGA and DTG curves.

increase to 28.2%, 30.6%, and 30.7%, respectively. For the UL-94 results, EP/CE/CuPP5 and EP/CE/CuPP7 composites achieve UL-94 V-1 rating.

Based on the results of LOI and UL-94, it can be inferred that the incorporation of CuPP improves flame retardancy of EP/CE copolymer. However, the observed improvement in flame retardancy tends to level off at CuPP concentration of 5 wt% or higher, which may be due to the worse dispersion of the flame retardant in the resin matrix, leading to some agglomeration of particles.

3.2.2 Cone calorimeter study

To gain a better understanding of the fire behavior of EP/CE/CuPP, we conducted forced flaming combustion studies using the CCT. CCT is widely recognized as a scientific method to study material burning behavior under conditions of developing fire scenarios. The related results are presented in Figure 2 and Table 3.

According to reference (25), the heat release rate (HRR) curve of all samples exhibits thermally thick

Table 2: LOI values and UL-94 ratings of EP/CE and its composites

Sample code	LOI (%)	UL-94 rating
Pure EP/CE	25.7 ± 0.2	NR*
EP/CE/CuPP3	28.2 ± 0.2	NR
EP/CE/CuPP5	30.6 ± 0.1	V-1
EP/CE/CuPP7	30.7 ± 0.1	V-1

*No rating.

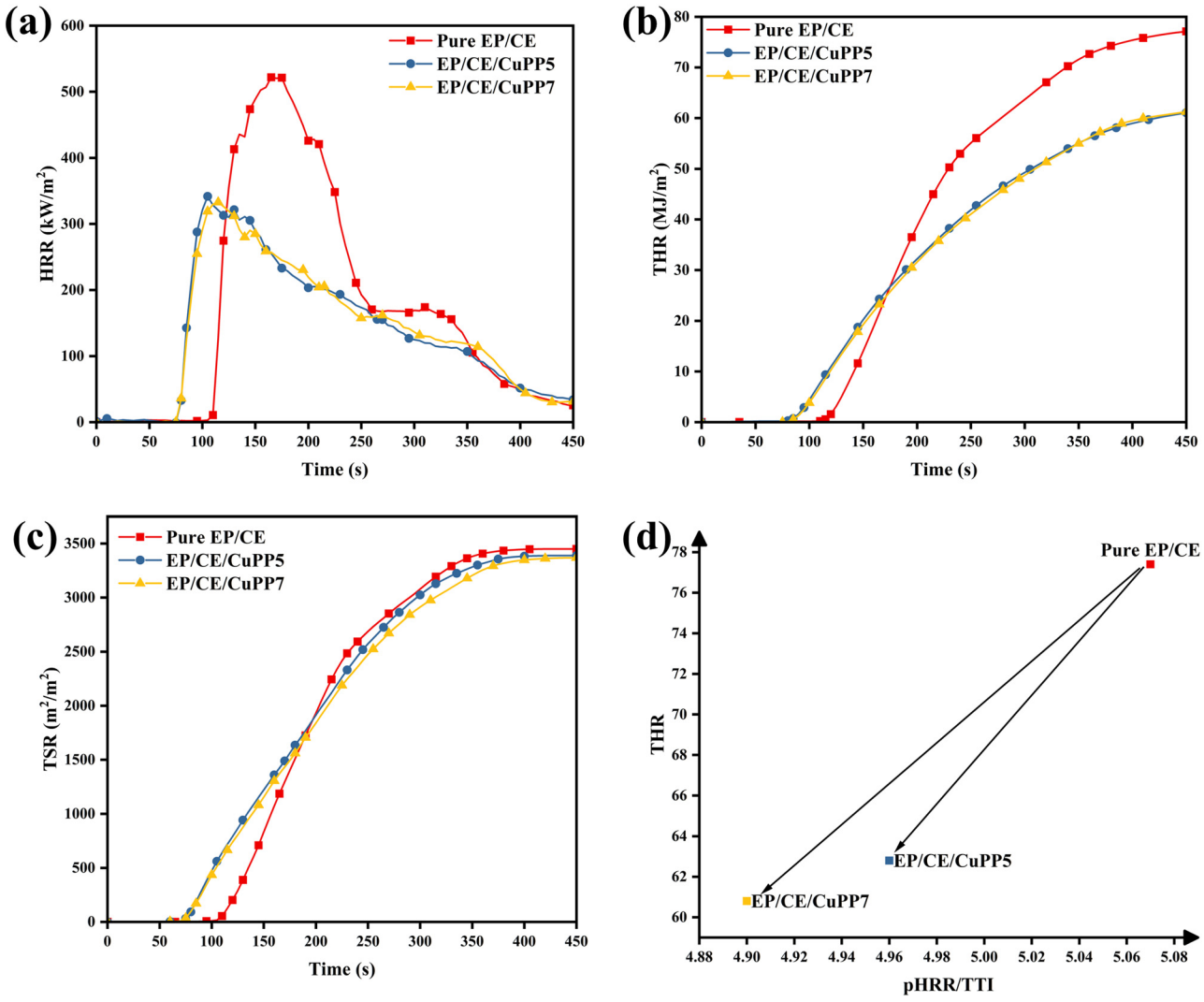

Figure 2: CCT results of EP/CE and its composites: (a) HRR, (b) THR, (c) TSR, and (d) THR-pHRR/TTI.

charring pattern. After ignition, the HRR of pure EP/CE rapidly ascends to its first peak and then gradually decreases over time due to the barrier effect of the char layer. At 300–350 s, a second weak peak appears, which is attributed to a fragile and broken carbon layer, resulting in a thermally thick non-charring situation. In contrast, the addition of CuPP has resulted in a notable advancement in the time to ignition (TTI), which is possibly due to the early decomposition of the matrix caused by CuPP. Compared with pure EP/CE, the composite containing 5 wt% CuPP exhibits a significant reduction of peak of heat release rate (pHRR) up to 34%, with the second peak disappearing, indicating that CuPP has a strengthening effect on the char layer, which corresponds to the increase of residue yield.

According to Petrella (26), the total heat release (THR) is plotted against the pHRR/TTI ratio (Figure 2d).

Table 3: CCT results of EP/CE and its composites

Sample code	TTI (s)	pHRR ($kW \cdot m^{-2}$)	THR ($MJ \cdot m^{-2}$)	EHC ($MJ \cdot kg^{-1}$)	TSR ($m^2 \cdot m^{-2}$)	Residue (wt%)
Pure EP/CE	103 ± 3	522 ± 32	77.4 ± 3.4	21.0 ± 2.5	3,440 ± 148	19.0 ± 0.7
EP/CE/CuPP5	69 ± 4	342 ± 28	62.8 ± 2.3	17.1 ± 2.0	3,363 ± 103	22.8 ± 0.4
EP/CE/CuPP7	68 ± 3	333 ± 6	60.8 ± 2.6	16.9 ± 2.7	3,335 ± 180	23.7 ± 1.1

The horizontal axis represents the propensity for a fire to spread rapidly, while the vertical axis measures the propensity for a prolonged fire. This graphical representation provides a clear and concise means of assessing fire risk. It is found that the incorporation of CuPP into the EP/CE has resulted in a reduction of both the THR and pHRR/TTI values. This reduction may be attributed to two reasons. First, the presence of CuPP serves to dilute the combustible content of the composite. Second, the char layer formed by burning EP/CE/CuPP is stronger than that of pure EP/CE, thus improving its fire performance.

The average effective heat of combustion (EHC) is a critical parameter for evaluating the activity of a flame retardant in the gas phase (27). It can be observed that the EHC of EP/CE/7CuPP exhibits a reduction of approximately 20% in comparison to that of pure EP/CE, suggesting that CuPP can exert a flame-retardant effect in the gas phase. Meanwhile, the total smoke release (TSR) values of the EP/CE/CuPP composites remain nearly unchanged.

3.2.3 Char analysis

The SEM images and macroscopic appearance of the residual chars of pure EP/CE and EP/CE/CuPP5 after CCT are shown in Figure 3.

Table 4: Element compositions of the residual char of pure EP/CE and EP/CE/CuPP5

Sample code	Element composition (%)				
	C	N	O	P	Cu
Pure EP/CE	78.35	6.34	15.31	0	0
EP/CE/CuPP5	31.56	9.50	9.25	15.16	34.53

The residual char of pure EP/CE (Figure 3a) exhibits a broken and fragile appearance, and SEM image reveals a smooth surface but with large cracks. For EP/CE/CuPP5 (Figure 3b), the residue exhibits a grey-green lamellar structure on a macroscopic scale, and SEM image reveals many bubble-like protrusions on the compact and continuous residual char, which can act as a stable protective layer. To further investigate the elemental composition of the residues char, EDS is applied, and the results are presented in Figure 3 and Table 4. It can be observed that the residual char from pure EP/CE contains only C, O, and N, while the residue from CuPP/EP/CE5 contains P and Cu elements besides C, O, and N.

Moreover, Raman is used to study the residual chars to explore the graphitization degree of carbon layer (28). The Raman spectra of the residues of pure EP/CE and EP/CE/CuPP5 are shown in Figure 4. The I_D/I_G ratio from

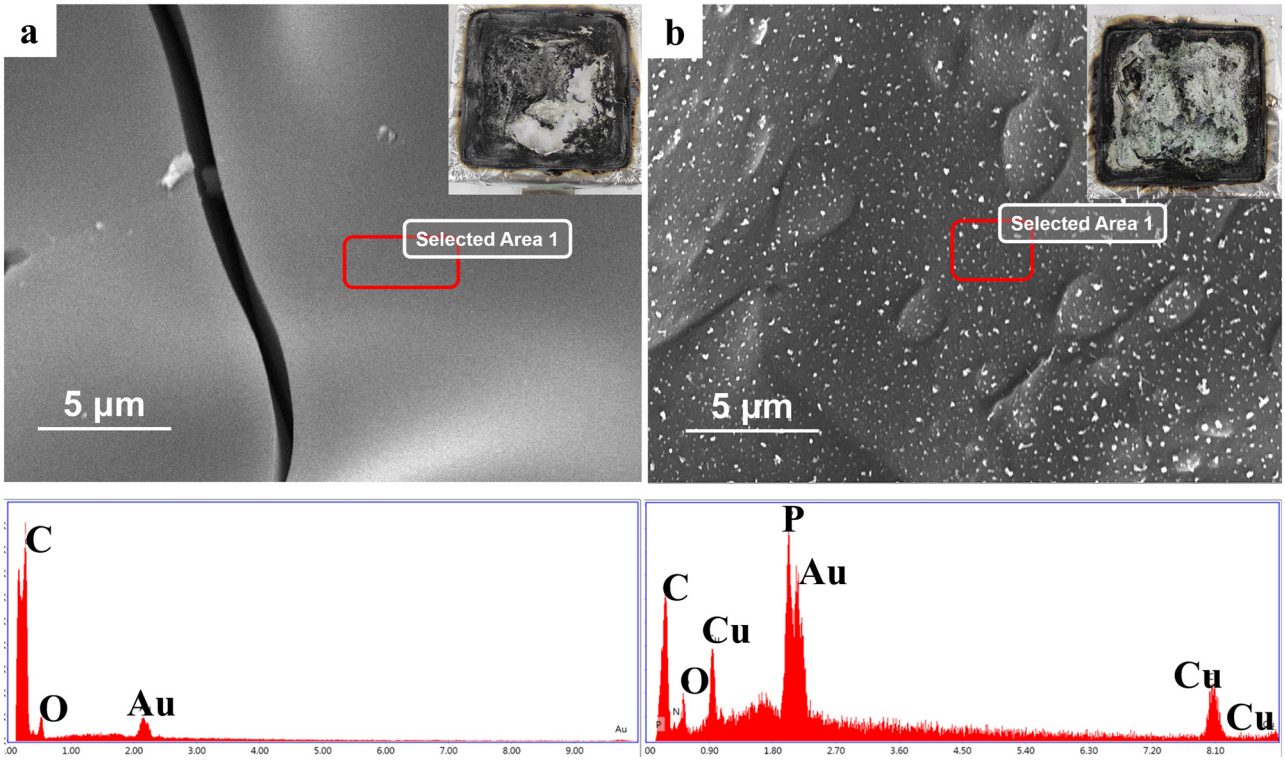

Figure 3: SEM, macroscopic appearance, and EDS spectra images of residual chars: (a) pure EP/CE and (b) EP/CE/CuPP5.

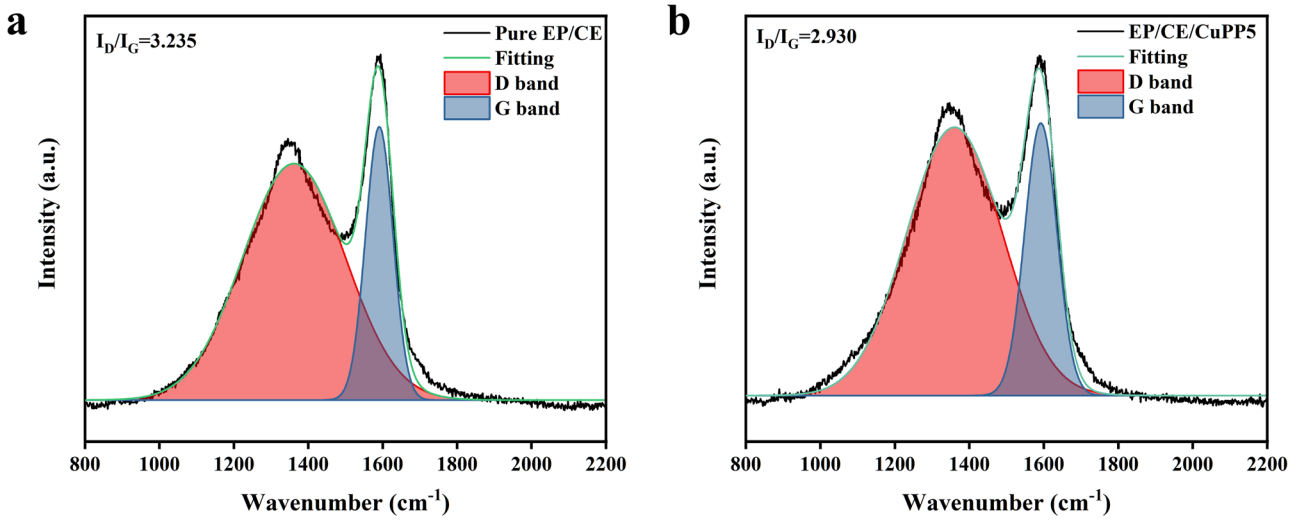

Figure 4: Raman spectra of residual chars: (a) pure EP/CE and (b) EP/CE/CuPP5.

pure EP/CE is 3.235, whereas the ratio from EP/CE/CuPP5 decreases to 2.930. The reduction in the ratio shows that the addition of CuPP improves the graphitization degree of the residual chars. This phenomenon probably results from the phosphorus-containing acid produced by the pyrolysis of CuPP and which can promote the formation of more ordered graphitized carbon (29).

Based on the analysis of the obtained data aforementioned, it can be inferred that the action of the flame retardant CuPP is predominantly exhibited within the condensed phase. During the combustion of the EP/CE/CuPP composites, CuPP decomposes to produce phosphorus-containing acids, which promote the matrix to form the carbonaceous char layer, which not only results in a reduction in the release of combustible volatiles but also prevents the transfer of heat and material between the condensed and gas phases.

3.3 Thermal behavior of EP/CE/CuPP composites

3.3.1 DSC study

The glass transition temperatures (T_g) of EP/CE and its composites are carried out by DSC and the curves are presented in Figure 5. The T_g of pure EP/CE is 211°C, while

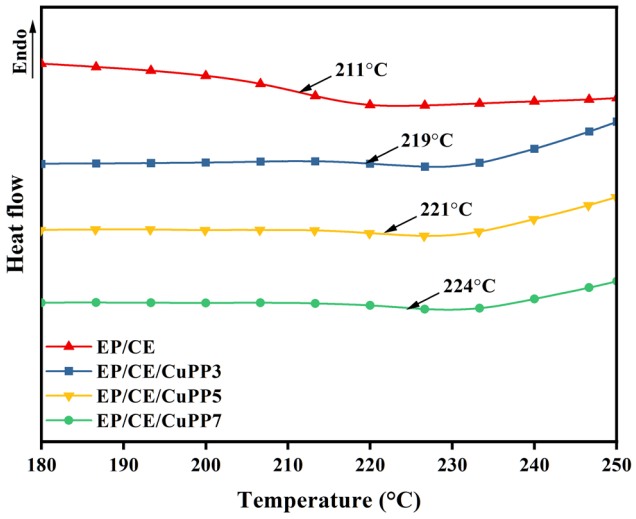

Figure 5: DSC curves of EP/CE and its composites.

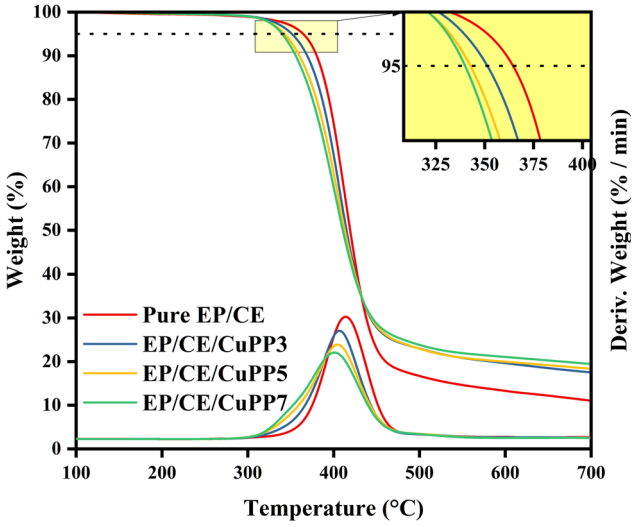

Figure 6: TGA curves of EP/CE and its composites.

Table 5: TGA results of EP/CE and its composites

Sample code	$T_{5\%}$ (°C)	T_{max} (°C)	Char residue at 700°C (wt%)
Pure EP/CE	364 ± 2	414 ± 2	11.0 ± 1.0
EP/CE/CuPP3	351 ± 3	407 ± 3	17.5 ± 1.5
EP/CE/CuPP5	342 ± 2	406 ± 2	18.4 ± 0.6
EP/CE/CuPP7	340 ± 2	400 ± 3	19.5 ± 1.1

the T_g values of the EP/CE/CuPP composites with 3, 5, and 7 wt% CuPP are 219, 221, and 224°C, respectively. The increase of T_g of the composites may be attributed to the presence of rigid CuPP nanosheets, which act as a physical crosslinking point within the EP/CE crosslinking network. The CuPP nanosheets prevent the movement of polymer molecular chains and reduces free volume, which lead to an increase in the network density and T_g (30,31).

3.3.2 TGA study

The TGA curves of EP/CE and its composites are shown in Figure 6 and the results are listed in Table 5. It is evident that all samples have one decomposition step. The temperature at 5 wt% weight loss ($T_{5\%}$) of pure EP/CE is 364°C, and the temperature at the maximum mass loss rate (T_{max}) appears at 414°C. For EP/CE/CuPP composites, due to the early decomposition of CuPP, $T_{5\%}$ and T_{max} values gradually drop with the increased addition of CuPP. The residue of pure EP/CE at 700°C is 11.0 wt% while the residues of EP/CE/CuPP are more than 15 wt%, which may be caused by the fact that the decomposition

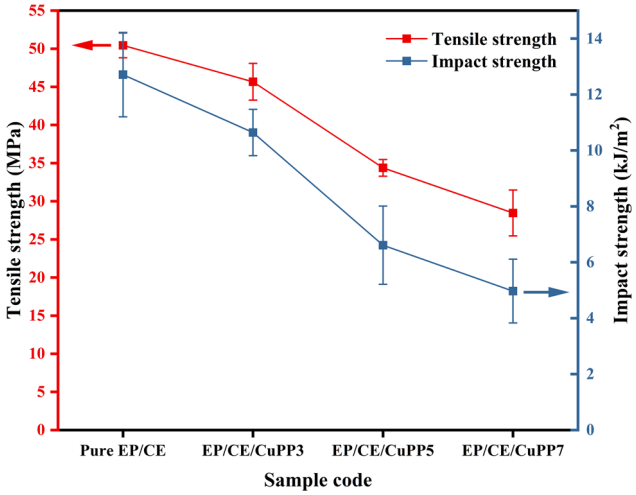

Figure 7: Mechanical properties of EP/CE and its composites.

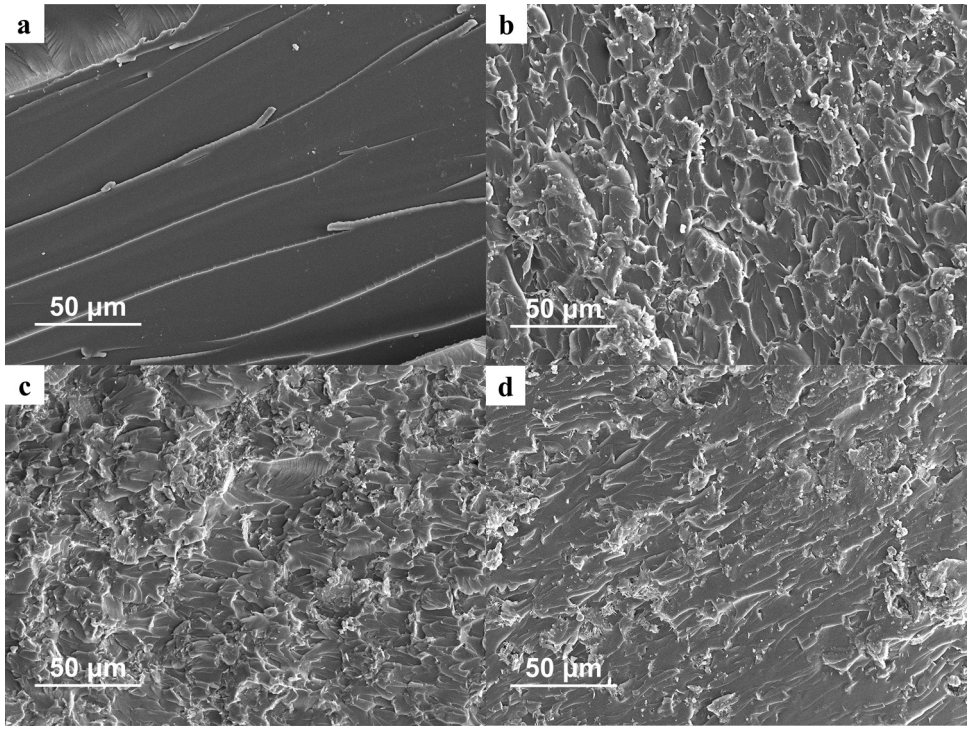

Figure 8: SEM images of fractured surfaces of EP/CE and its composites: (a) pure EP/CE, (b) EP/CE/CuPP3, (c) EP/CE/CuPP5, and (d) EP/CE/CuPP7.

products of CuPP are helpful to promote char formation of the resin.

3.4 Mechanical properties of EP/CE composites

The mechanical properties of EP/CE and its composites are shown in Figure 7. Although the T_g and network density of the composite increase with the addition of CuPP, the mechanical properties actually decrease instead. The decrease in the mechanical properties of EP/CE/CuPP composites is likely to be related to the high loading and the poor dispersion of CuPP particles in the matrix, resulting in stress concentration and deterioration in the mechanical properties (32).

To further explore the mechanism of adding CuPP on the mechanical properties of EP/CE copolymer, the microstructures of fractured surface of the composites are investigated by SEM. As shown in Figure 8a, pure EP/CE exhibits a typical brittle feature with many river-like cracks on the smooth surface. The fractured surfaces of the EP/CE/CuPP composites (Figure 8b–d) with a lot of layered protrusions and tough whirls are much coarser than that of pure sample. The layered protrusions and tough whirls can absorb energy during finite cracks propagation, thereby raising the toughness and preventing further damage of the materials, theoretically. However, many cavitation produced by particle peeling is observed from the fractured surface of the EP/CE/CuPP composites, which can be contributed to the local stress concentration after the incorporation of CuPP and thus deterioration of mechanical performance of the composites.

4 Conclusion

In this work, CuPP, a novel flame retardant, was facilely synthesized and confirmed by FTIR, XRD, TGA, and TEM. EP/CE composites with CuPP were successfully prepared as well, and the effects of the CuPP on flame retardancy, thermal resistance and mechanical properties of the EP/CE composites were studied. The EP/CE/CuPP5 composite showed the outstanding flame retardancy with a LOI of 30.6% and UL-94 V-1 rating. The PHRR and THR values of EP/CE/CuPP5 decrease by 34.5% and 18.9%, respectively, compared with those of samples without CuPP. SEM, EDS, and Raman spectra of residues prove that CuPP exerts its flame-retardant role in the EP/CE copolymer mainly in the condensed phase. The T_g values of the EP/CE/CuPP composites are all higher than the one of pure EP/CE, but the introduction of CuPP leads to a decrease in mechanical properties of EP/CE/CuPP composites.

Funding information: This work was financially supported by the National Natural Science Foundation of China (21975185).

Author contributions: Zhilin Cao: writing – original draft, writing – review and editing, visualization, investigation, formal analysis; Changxin Ren: writing – original draft, investigation, conceptualization; Zhengzhou Wang: supervision, project administration.

Conflict of interest: The authors state no conflict of interest.

Data availability statement: The data sets generated during and/or analyzed during the current study are available from the corresponding author on reasonable request.

References

(1) Chen Y, Li Z, Liu Y, Teng C, Cui W. Curing mechanism and mechanical properties of Al_2O_3/cyanate ester–epoxy composites. J Electron Mater. 2020;49(2):1473–81. doi: 10.1007/s11664-019-07836-w.

(2) Zhang X, Wang F, Zhu Y, Qi H. Cyanate ester composites containing surface functionalized BN particles with grafted hyperpolyarylamide exhibiting desirable thermal conductivities and a low dielectric constant. RSC Adv. 2019;9(62):36424–33. doi: 10.1039/C9RA06753A.

(3) Chen Y, Li Z, Liu Y, Teng C, Cui W. Effect of Al_2O_3 on microstructure and dielectric properties of epoxy-cyanate ester composite material. J Mater Sci: Mater Electron. 2019;30(23):20614–23. doi: 10.1007/s10854-019-02427-1.

(4) Chandramohan A, Dinkaran K, Kumar AA, Alagar M. Synthesis and characterization of epoxy modified cyanate ester POSS nanocomposites. High Perform Polym. 2012;24(5):405–17. doi: 10.1177/0954008312441640.

(5) Lei Y, Xu M, Jiang M, Huang Y, Liu X. Curing behaviors of cyanate ester/epoxy copolymers and their dielectric properties. High Perform Polym. 2017;29(10):1175–84. doi: 10.1177/0954008316672291.

(6) Liu Z, Yuan L, Liang G, Gu A. Tough epoxy/cyanate ester resins with improved thermal stability, lower dielectric constant and loss based on unique hyperbranched polysiloxane liquid crystalline: Cyanate Ester Resins with Hyperbranched Polymer Liquid Crystalline. Polym Adv Technol. 2015;26(12):1608–18. doi: 10.1002/pat.3590.

(7) Kim BS. Effect of cyanate ester on the cure behavior and thermal stability of epoxy resin. J Appl Polym Sci. 1997;65(1):85–90. doi: 10.1002/(SICI)1097-4628(19970705)65:1<85:AID-APP11>3.0.CO;2-Y.
(8) Jayakumari LS, Thulasiraman V, Sarojadevi M. Synthesis and characterization of cyanate epoxy composites. High Perform Polym. 2007;19(1):33–47. doi: 10.1177/0954008306072147.
(9) Liang G, Zhang M. Enhancement of processability of cyanate ester resin via copolymerization with epoxy resin. J Appl Polym Sci. 2002;85(11):2377–81. doi: 10.1002/app.10872.
(10) Lin CH. Synthesis of novel phosphorus-containing cyanate esters and their curing reaction with epoxy resin. Polymer. 2004;45(23):7911–26. doi: 10.1016/j.polymer.2004.09.023.
(11) Preston CML, Amarasinghe G, Hopewell JL, Shanks RA, Mathys Z. Evaluation of polar ethylene copolymers as fire retardant nanocomposite matrices. Polym Degrad Stab. 2004;84(3):533–44. doi: 10.1016/j.polymdegradstab.2004.02.004.
(12) Ho T, Hwang H, Shieh J, Chung M. Thermal, physical and flame-retardant properties of phosphorus-containing epoxy cured with cyanate ester. React Funct Polym. 2009;69(3):176–82. doi: 10.1016/j.reactfunctpolym.2008.12.019.
(13) Toldy A, Szlancsik Á, Szolnoki B. Reactive flame retardancy of cyanate ester/epoxy resin blends and their carbon fibre reinforced composites. Polym Degrad Stab. 2016;128:29–38. doi: 10.1016/j.polymdegradstab.2016.02.015.
(14) Wang Z, Gao X, Li W. Epoxy resin/cyanate ester composites containing DOPO and wollastonite with simultaneously improved flame retardancy and thermal resistance. High Perform Polym. 2020;32(6):710–8. doi: 10.1177/0954008319897095.
(15) Toldy A, Niedermann P, Szebenyi G, Szolnoki B. Mechanical properties of reactively flame retarded cyanate ester/epoxy resin blends and their carbon fibre reinforced composites. Express Polym Lett. 2016;10(12):1016–25. doi: 10.3144/expresspolymlett.2016.94.
(16) Müller P, Schartel B. Melamine poly(metal phosphates) as flame retardant in epoxy resin: Performance, modes of action, and synergy. J Appl Polym Sci. 2016;133(24):43549–62. doi: 10.1002/app.43549.
(17) Liu L, Huang Y, Yang Y, Ma J, Yang J, Yin Q. Preparation of metal-phosphorus hybridized nanomaterials and the action of metal centers on the flame retardancy of epoxy resin. J Appl Polym Sci. 2017;134(48):45445–55. doi: 10.1002/app.45445.
(18) Wang W, Wang Z. Flame retardancy, thermal decomposition and mechanical properties of epoxy resin modified with copper N, N'-piperazine (bismethylene phosphonate). J Therm Anal Calorim. 2022;147(3):2155–69. doi: 10.1007/s10973-021-10592-x.
(19) Zhou T, Wu T, Xiang H, Li Z, Xu Z, Kong Q, et al. Simultaneously improving flame retardancy and dynamic mechanical properties of epoxy resin nanocomposites through synergistic effect of zirconium phenylphosphate and POSS. J Therm Anal Calorim. 2019;135(4):2117–24. doi: 10.1007/s10973-018-7387-4.
(20) Xie J, Chang J, Wang X. Application of infrared spectroscopy in organic chemistry and pharmaceutical chemistry. revised ed. Beijing: Science Press; 2001.
(21) Hayashi H, Hudson MJ. Reaction of the phenyiphosphonate anion with the layered basic copper(II) nitrate $[Cu_2(OH)_3NO_3]$. J Mater Chem. 1995;5(1):115–9. doi: 10.1039/jm9950500115.
(22) Kong Q, Wu T, Zhang J, Wang DY. Simultaneously improving flame retardancy and dynamic mechanical properties of epoxy resin nanocomposites through layered copper phenylphosphate. Compos Sci Technol. 2018;154:136–44. doi: 10.1016/j.compscitech.2017.10.013.
(23) Yucesan G, Yu MH, Ouellette W, O'Connor CJ, Zubieta J. Secondary metal–ligand cationic subunits $\{ML\}^{n+}$ as structural determinants in the oxovanadium/phenylphosphonate/$\{ML\}^{n+}$ system, where $\{ML\}$ is a Cu^{2+}/organonitrogen moiety. Cryst Eng Comm. 2005;7(80):480–90. doi: 10.1039/b506250k.
(24) Wang J, Yuan B, Mu X, Feng X, Tai Q, Hu Y. Two-dimensional metal phenylphosphonates as novel flame retardants for polystyrene. Ind Eng Chem Res. 2017;56(25):7192–206. doi: 10.1021/acs.iecr.7b00858.
(25) Schartel B, Hull TR. Development of fire-retarded materials—Interpretation of cone calorimeter data. Fire Mater. 2007;31(5):327–54. doi: 10.1002/fam.949.
(26) Petrella RV. The Assessment of Full-Scale Fire Hazards from Cone Calorimeter Data. J Fire Sci. 1994;12(1):14–43. doi: 10.1177/073490419401200102.
(27) Schartel B, Braun U. Comprehensive fire behaviour assessment of polymeric materials based on cone calorimeter investigations. e-Polymers. 2003;3(1):177–90. doi: 10.1515/epoly.2003.3.1.177.
(28) Sadezky A, Muckenhuber H, Grothe H, Niessner R, Pöschl U. Raman microspectroscopy of soot and related carbonaceous materials: Spectral analysis and structural information. Carbon. 2005;43(8):1731–42. doi: 10.1016/j.carbon.2005.02.018.
(29) Qian X, Song L, Jiang S, Tang G, Xing W, Wang B, et al. Novel Flame Retardants Containing 9,10-Dihydro-9-oxa-10-phosphaphenanthrene-10-oxide and unsaturated bonds: synthesis, characterization, and application in the flame retardancy of epoxy acrylates. Ind Eng Chem Res. 2013;52(22):7307–15. doi: 10.1021/ie400872q.
(30) Chen Y, Chen E, Wu T. Organically modified layered zinc phenylphosphonate reinforced stereocomplex-type poly(lactic acid) nanocomposites with highly enhanced mechanical properties and degradability. J Mater Sci. 2015;50(23):7770–8. doi: 10.1007/s10853-015-9348-7.
(31) Kong Q, Sun Y, Zhang C, Guan H, Zhang J, Wang DY, et al. Ultrathin iron phenyl phosphonate nanosheets with appropriate thermal stability for improving fire safety in epoxy. Compos Sci Technol. 2019;182:107748–57. doi: 10.1016/j.compscitech.2019.107748.
(32) Zhang Z, Liang G, Wang X. Epoxy-functionalized polyhedral oligomeric silsesquioxane/cyanate ester resin organic-inorganic hybrids with enhanced mechanical and thermal properties: Epoxy functionalized POSS/cyanate ester resin hybrids. Polym Int. 2014;63(3):552–9. doi: 10.1002/pi.4557.